nature materials

LETTERS

PUBLISHED ONLINE: 24 JULY 2011 | DOI: 10.1038/NMAT3078

Nucleation mechanism for the direct graphite-to-diamond phase transition

Rustam Z. Khaliullin[1]*, Hagai Eshet[1], Thomas D. Kühne[2,3], Jörg Behler[4] and Michele Parrinello[1]

Graphite and diamond have comparable free energies, yet forming diamond from graphite in the absence of a catalyst requires pressures that are significantly higher than those at equilibrium coexistence[1–7]. At lower temperatures, the formation of the metastable hexagonal polymorph of diamond is favoured instead of the more stable cubic diamond[2,5–7]. These phenomena cannot be explained by the concerted mechanism suggested in previous theoretical studies[8–12]. Using an *ab initio* quality neural-network potential[13], we carried out a large-scale study of the graphite-to-diamond transition assuming that it occurs through nucleation. The nucleation mechanism accounts for the observed phenomenology and reveals its microscopic origins. We demonstrate that the large lattice distortions that accompany the formation of diamond nuclei inhibit the phase transition at low pressure, and direct it towards the hexagonal diamond phase at higher pressure. The proposed nucleation mechanism should improve our understanding of structural transformations in a wide range of carbon-based materials.

Static compression of hexagonal graphite (HG) results in the formation of metastable hexagonal diamond (HD) at temperatures $T \sim 1,200$–$1,700$ K (refs 2,5–7) and cubic diamond (CD) at higher temperatures[1,3–5,7]. Although the transition pressure is sensitive to the nature of the graphite samples, neither of the diamond phases has been observed to form below ∼12 GPa. This pressure is significantly higher than the graphite–diamond coexistence pressure approximated by the Berman–Simon line $P\,(\mathrm{GPa}) \sim 0.76 + 2.78 \times 10^{-3} T\,(\mathrm{K})$ (ref. 14).

Despite being an area of intense theoretical research[8–12], the microscopic mechanism of the formation of metastable HD and the reason for the remarkable stability of graphite above the coexistence pressure are still unknown. Computer simulations, which could help resolve these issues, have been hindered because of the inability of empirical potentials to describe the energetics of the transformation accurately[13,15] and the computational expense of more reliable *ab initio* molecular dynamics. In the latter case, short simulation time and small system size (that is, several hundred atoms) force the transition to occur in a concerted manner with the ultrafast (∼10^{-2}–1 ps) synchronous formation of all new chemical bonds across the entire simulation box[11,12,16]. Whereas concerted mechanisms can be observed at shock compression[16–18], the transformation under static conditions is expected to proceed through nucleation and growth.

It has been estimated that, because diamond has an extremely high surface energy[19], its critical nuclei may contain thousands of atoms[20–22]. Hence, tens or even hundreds of thousands of atoms are required to model the diamond nuclei and the surrounding graphite matrix. Direct *ab initio* simulations of systems of this size are outright impossible. Therefore, theoretical studies of the nucleation have been restricted to simple continuum models[20–22], which ignore the anisotropic nature of graphite, use significantly different estimates of the surface energy terms and ignore the distortion of graphite around the growing nuclei.

In recent works, we have demonstrated that high-dimensional neural networks (NNs; ref. 23) are capable of creating accurate representations of *ab initio* potential-energy surfaces of numerous elements[13,23,24]. Even in the case of graphite and diamond, which are very differently bonded, a NN potential predicts all relevant properties in quantitative agreement with *ab initio* and experimental data (see Methods and ref. 13). Furthermore, the computational efficiency of molecular dynamics based on the NN potential enables us to extend time and length scales accessible to simulations and, thus, to carry out the first atomistic study of homogeneous diamond nucleation from graphite.

The energetics of the nucleation was studied at zero temperature by seeding diamond nuclei of various sizes inside a periodic ∼100 Å × 100 Å × 100 Å graphite matrix containing ∼145,000 atoms (see Methods). Hexagonal and rhombohedral graphite (RG) lattices were used as initial structures for the formation of HD and CD nuclei, respectively, because of the high symmetry of the HG → HD and RG → CD transformation pathways[8,10]. HD and CD nuclei were formed by shifting atoms in the graphite lattice in the manner shown in Fig. 1a. Buckling of basal planes into the 'chair' conformation in the RG lattice leads to CD, whereas the 'boat' buckling of the HG lattice results in the formation of HD. Such distortions of graphite planes have been observed in previous *ab initio* simulations[11] and satisfy the orientation relations between graphite and diamond crystals discovered experimentally[2,5,7,25]:

$$(100)_{\mathrm{HD}} \parallel (001)_{\mathrm{G}} \text{ and } [100]_{\mathrm{HD}} \parallel [100]_{\mathrm{G}}$$

$$(111)_{\mathrm{CD}} \parallel (001)_{\mathrm{G}} \text{ and } [110]_{\mathrm{CD}} \parallel [100]_{\mathrm{G}}$$

Our calculations show that the nucleation process is strongly influenced by pressure. Both the nucleation barrier and the size of the critical nuclei decrease rapidly as the pressure is increased (Figs 2 and 3). Examination of the atomic structure of the diamond nuclei reveals the microscopic origin of this phenomenon. Diamond nuclei are generally highly non-spherical and contain a diamond core (red atoms in Fig. 2) separated from a relaxation region of the graphite lattice by a thin (∼5 Å) high-enthalpy interface. To form interlayer bonds in the core, large regions in a number of graphite layers have to be buckled and bent in the $[001]_{\mathrm{G}}$ direction.

[1]Department of Chemistry and Applied Biosciences, ETH Zürich, USI Campus, via G. Buffi 13, 6900 Lugano, Switzerland, [2]Institute of Physical Chemistry, Johannes Gutenberg University Mainz, D-55128 Mainz, Germany, [3]Center for Computational Sciences, Johannes Gutenberg University Mainz, D-55128 Mainz, Germany, [4]Lehrstuhl für Theoretische Chemie, Ruhr-Universität Bochum, D-44780 Bochum, Germany. *e-mail: rustam@khaliullin.com.

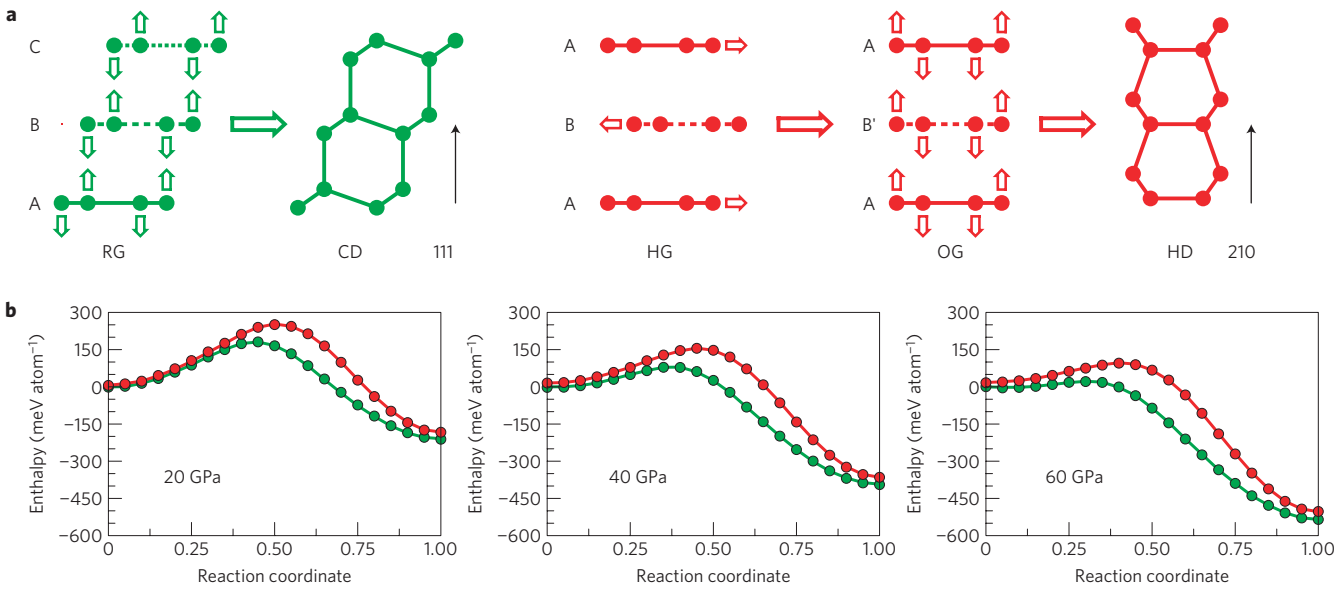

Figure 1 | Concerted transformation of graphite to diamond. a, Pathways for RG → CD (green) and HG → HD (red) transformations. OG denotes an (unstable) intermediate orthorhombic graphite phase. **b**, Density functional theory (DFT; lines) and NN (circles) enthalpy profiles for the concerted mechanism: RG → CD (green) and OG → HD (red). The enthalpy of undistorted RG is taken as zero.

At low pressure, these distortions are energetically costly because of the significant mismatch between the $[001]_G$ lattice parameters of the parent phase and the nuclei (for example, the energetic cost of forming the unit graphite–diamond interface in the $[001]_G$ direction is shown in Fig. 4a). At 10 GPa, we did not observe the formation of interlayer bonds even around large diamond seeds. At higher pressure the mismatch decreases and the diamond cores become increasingly more spherical (Fig. 2). The same mismatch is the reason for the $[001]_G$ distortion of the graphite crystal around the nuclei. The extent of the distorted region decreases with the increase in pressure.

As the size of the distorted region around the diamond core grows linearly with the size of the core, the free energy of the diamond nucleus in graphite can be written as[26,27]

$$\Delta G = (\Delta g_s + \Delta g_\mu)V + \sigma S$$

where Δg_μ is the difference between the free-energy densities of bulk diamond and graphite, Δg_s is the positive misfit-strain free energy per nucleus volume and σ is the interfacial free-energy density. S and V are the surface area and volume of the nucleus, respectively. Owing to the considerable mismatch between the lattice parameters, the large strain-energy term outweighs the relatively small bulk term at $P < 10$ GPa and makes nucleation impossible (that is, the volume term becomes positive). As a result, the 10 GPa nucleation curve does not show any signs of flattening out even for a nucleus size of 100 Å. In contrast, the 20 GPa curve is predicted to reach the maximum around 25–31 Å and 560–630 eV. Hence, our results are consistent with the observed ~12 GPa minimum pressure threshold for diamond formation. The negative bulk term Δg_μ increases in magnitude with pressure (Fig. 1b), whereas the positive strain term becomes smaller (note the extent of the relaxation region around the diamond core in Fig. 2), leading to the observed decrease in the nucleation barriers (Fig. 3).

Comparison of the transition barriers for the concerted pathways and the nucleation process (Table 1) shows that the nucleation is energetically more favourable in the pressure range used in compression experiments. Hence, nucleation represents a more realistic mechanism for diamond formation. However, at higher pressure the graphite crystal approaches the lattice instability point and the activation barriers for the continuous transformations are lower (Fig. 1b and Table 1). In this high-pressure limit, diamond domains can appear spontaneously throughout the graphite matrix without the formation of a well-defined graphite–diamond interface. For example, at 60–70 GPa, the formation of only a few interlayer bonds in close proximity to one another is enough to initiate rapid irreversible growth of a diamond crystal.

Table 1 | Comparison of the enthalpy barriers of the concerted pathways and nucleation.

Pressure (GPa)	Nucleation* (meV atom^{-1})	Concerted (meV atom^{-1}) CD†	HD†
30	70–90	130	185
40	40–60	80	140
50	110–280	50	93

*Calculated by dividing the nucleation barrier by the number of atoms in the diamond core ($\chi_i > 0.8$) of the critical nucleus. This value gives the upper bound on the nucleation barrier.
†Pathways are shown in Fig. 1a with green (CD) and red (HD) colours.

It is worth noting that homogeneous nucleation represents an idealized model of the real nucleation process. Recent experiments demonstrate that highly ordered graphite exhibits lower rates of diamond synthesis than disordered graphite materials[28], implying that structural defects play an important role in the graphite-to-diamond transformation. Computer models have shown that dangling bonds around structural defects (for example, dislocation edges) can facilitate the creation of interlayer covalent bonds and thus lead to the formation of large regions of sp^3-hybridized atoms inside the graphite lattice[29]. Such domains of sp^3-hybridized atoms can serve as pre-existing nucleation sites and lower the nucleation barriers. Therefore, the barriers in Fig. 3, which are especially high at pressures of 20–30 GPa, represent an upper bound for the real nucleation barrier. Nevertheless, despite the importance of lattice defects in the transformation, the homogeneous nucleation model correctly captures the main features of the nucleation process. The energetics of lattice distortions around diamond nuclei are expected to be similar for homogeneous and heterogeneous nucleation

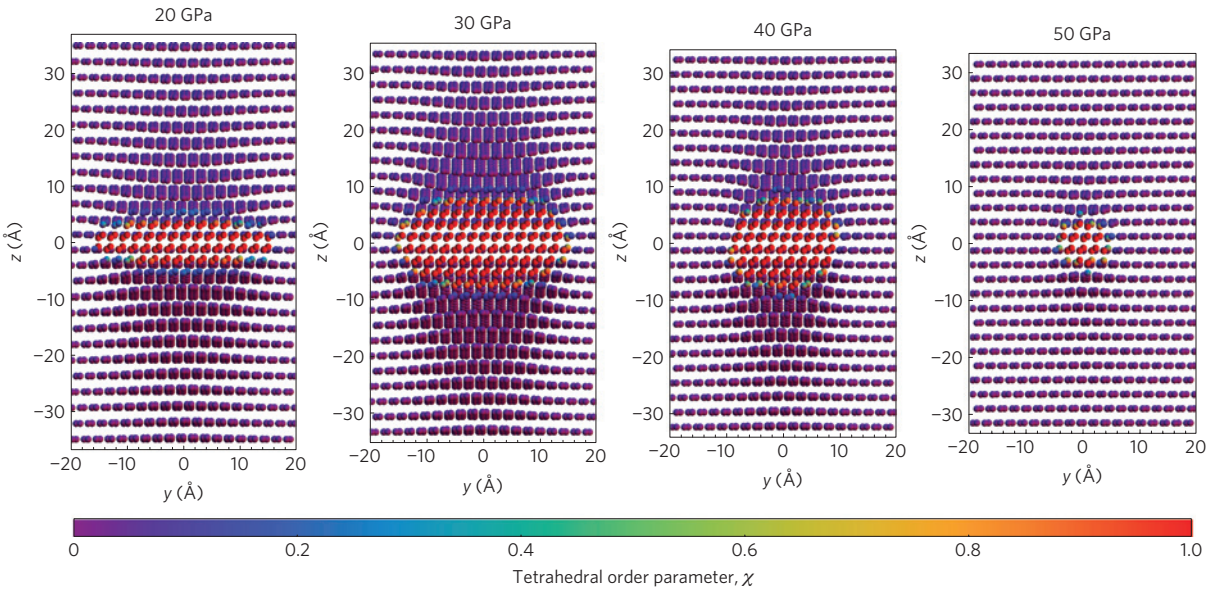

Figure 2 | Pressure dependence of the shape and size of CD nuclei. The optimized critical nuclei are shown for 30, 40 and 50 GPa whereas the 20 GPa nucleus is below the critical size and is presented to compare its shape with that of the 30 GPa nucleus. Atoms are coloured according to the values of the tetrahedral atomic order parameter defined to distinguish graphite ($\chi_i \sim 0$) and diamond ($\chi_i \sim 1$) configurations (see Methods).

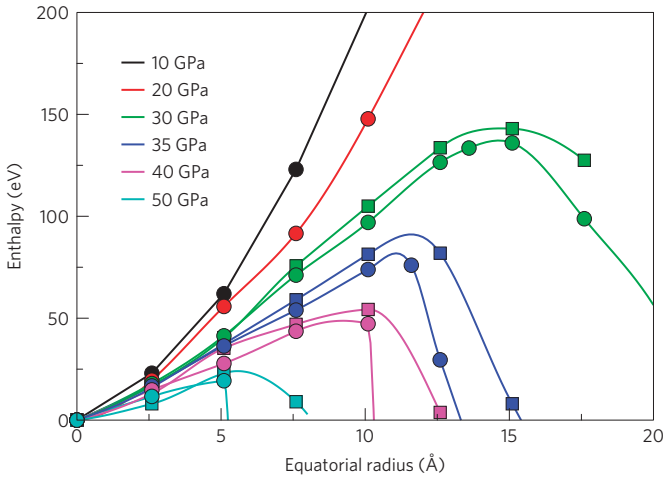

Figure 3 | Pressure dependence of the nucleation barriers for the RG → CD (circles) and HG → HD (squares) transformations. The 20 GPa curve is predicted to reach the maximum around 25–31 Å and 560–630 eV. The sharp drop of the curves at high pressure provides evidence that there are extremely low barriers for adding atoms to the critical nuclei that prevent stabilization of supercritical CD nuclei even at low temperatures.

and, thus, the diamond growth at defects will be governed by mechanisms similar to those described above.

The activation barriers for the concerted mechanism are determined by the energetics of buckling of graphite basal planes into the 'chair' or 'boat' configurations. The considerably lower activation barrier along the 'chair' buckling mode favours the formation of CD (Fig. 1b and Table 1), whereas in experiments the metastable HD phase is often observed. This disagreement between the theoretical predictions and experiment is resolved if the nucleation mechanism of diamond formation is considered. Our calculations show that the nucleation barriers for the HG → HD and RG → CD processes are not very different (Fig. 3). The similar heights of activation barriers are the consequence of comparable energies of the CD and HD nuclei and their surface energies.

In the nucleation process, the graphite basal planes undergo local 'in-layer' distortions that bring the atoms into an appropriate stacking sequence inside the diamond nuclei. The slightly higher barriers along the pathway leading to the HD phase are a consequence of this local $[210]_G$ distortion. This distortion brings the neighbouring layers from the hexagonal (AB) to orthorhombic (AB′) stacking (Fig. 1a) inside the HD nuclei. The HG → CD nucleation process is considerably more difficult than both the RG → CD and HG → HD nucleations. The strains necessary to distort the lattice from the AB stacking in HG to ABC stacking inside CD nuclei prevent stabilization of the CD nuclei inside the HG lattice in our simulations.

In-layer distortions have not been observed in any of the previous theoretical studies of this phase transition[11,12,16], because in-layer stresses result in the artificial sliding of graphite layers in small-cell simulations. Our results suggest that the in-layer distortions in large-cell simulations determine the energetics of the transformation and the overall direction for the phase transition. The higher in-layer strains for the HG → HD transformation relative to the HG → CD transition explain why HD is formed from graphite, which mostly consists of the hexagonal form. On the other hand, our studies show that the formation of CD is favoured in the RG lattice because no in-layer distortions are required for the RG → CD process. This implies that CD nucleates in the HG samples around stacking faults (for example $[AB]_n[CA]_m$), which are common defects in the HG lattice. High-temperature fluctuations can also activate the sliding of graphite basal planes in HG with the formation of the RG regions and, hence, favour the nucleation of the CD phase.

In conclusion, our study of diamond nucleation offers new insights into the atomistic mechanism for the direct graphite-to-diamond phase transition. We have demonstrated that the transformation does not occur at the graphite–diamond co-existence pressure in the static compression experiments because of the prohibitively large strains accompanying the formation of diamond nuclei. We have also shown that, at higher pressures, the nucleation mechanism is favoured over the concerted transformation. Larger distortions of the graphite lattice around the CD nuclei compared to those around the HD nuclei explain the formation of the metastable HD phase. At yet higher pressures, the transition

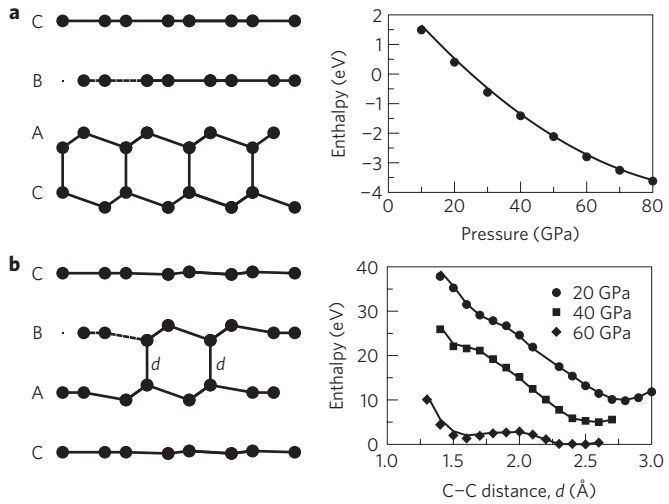

Figure 4 | Comparison of the NN and DFT energetics for mixed graphite–diamond systems. a, DFT (line) and NN (circles) enthalpies of the $[001]_G$ graphite–diamond interface (relative to RG). **b**, DFT (lines) and NN (symbols) enthalpy profiles for a nucleation pathway of CD. The enthalpy of undistorted RG is taken as zero; the 20 and 40 GPa curves are shifted up for clarity.

is continuous and proceeds without formation of a well-defined graphite–diamond interface.

The high barriers calculated for homogeneous nucleation also imply that structural defects in the graphite lattice might play an important role in the phase transformation. To reveal the extent of the influence of the dimensionality and detailed structure of various defect seeds on the energetics of the transition, a finite temperature molecular dynamics study of the thermodynamics and kinetics for heterogeneous nucleation will be carried out in the future. The computational and theoretical models presented here offer new opportunities for investigation of complex structural transformations in a wide range of carbon-based materials.

Methods

The NN potential was optimized to reproduce the Perdew–Burke–Ernzerhof density functional[30] energies for the relevant carbon structures in the pressure range up to 100 GPa. As described in our previous paper[13], the Perdew–Burke–Ernzerhof functional in combination with a dispersion-corrected atom-centred pseudopotential[31] accounts for the van der Waals interactions in graphite and describes experimental structural, elastic and vibrational properties of the diamond and graphite phases. The ABINIT package was used to obtain the reference *ab initio* energies. A dense mesh of k points and a large plane-wave cutoff of 170 Ry were used for all structures to ensure convergence of the total energy to 1.5 meV atom^{-1}.

The NN potential optimized for high-pressure high-temperature graphite and diamond in the previous work[13] was extended to reproduce the energetics of the transformations between the two phases. To this end, structures lying on high-symmetry transformation pathways (Supplementary Fig. S1) were included in the training set. After this, the NN was further refined using the *ab initio* energies of configurations of various graphite–diamond interfaces that emerged in the preliminary NN-driven optimization of the nuclei (Supplementary Fig. S2). The NN fitting procedure introduces only a small error (the root mean square error of the independent test sets is 4.0 meV atom^{-1}) in addition to the numerical (convergence) error of the DFT calculations. Thus, the NN potential is expected to describe the nucleation process of diamond from graphite with an accuracy comparable to that of the Perdew–Burke–Ernzerhof functional.

Figure 1b shows that the energetics of concerted transformations in small cells obtained with the NN potential is indistinguishable from the DFT results. In quantitative agreement with the *ab initio* calculations of ref. 10, the stability of diamond relative to graphite increases with pressure, whereas the barrier separating the two phases decreases. At a pressure of 80 GPa graphite reaches a lattice instability point (that is, one of the barriers becomes zero) and undergoes an ultrafast transformation to diamond as was previously observed in *ab initio* simulations in ref. 11 The NN-driven molecular dynamics simulations at constant pressure and temperature correctly reproduce the mechanism of this concerted transformation and are in perfect agreement with the results of ref. 11. Figure 4 demonstrates that the energy of the graphite–diamond interface and the formation of a small diamond nucleus in a system of ∼100 atoms is also excellently described by the NN.

The energetics of the nucleation of diamond from graphite was studied at zero temperature on a model system of 145,152 carbon atoms arranged in a graphite lattice in a periodic $\sim 100 \times 100 \times 100$ Å simulation cell. Diamond nuclei of various shapes and sizes were seeded by shifting atoms within a certain predefined region of the cell in the directions shown in Fig. 1a and constraining distances between appropriate pairs of atoms to the values corresponding to the C–C distance in diamond. RG and HG were used as a starting lattice for the formation of CD and HD nuclei, respectively. 30 ps constant-pressure molecular dynamics simulations at 1,000 K were carried out to relax the atoms around the constrained region followed by quenching to zero temperature. Finally, the constraints were removed and the geometry was optimized at constant pressure to obtain fully relaxed nuclei. We found that regardless of the shape of the initial constrained region all relaxed nuclei have shapes similar to those shown in Fig. 2. We verified that all simulation results are converged with respect to the system size by carrying out further test calculations for a $\sim 200 \times 200 \times 200$ Å simulation cell.

The tetrahedral order parameter χ_i for atom i is defined as follows: $\chi_i = (72/n_i(n_i-1))\sum_{j>k} n_{ij}n_{ik}((1/2)+\cos\theta_{jik})^2$, where the cutoff function is $n_{ij} = [1+e^{(r_{ij}-r_0)/\Delta r}]^{-1}$, the atom coordination number is $n_i = \sum_j n_{ij}$ and $r_0 = 1.6$ Å, $\Delta r = 0.005$ Å.

Received 4 January 2011; accepted 22 June 2011; published online 24 July 2011

References

1. Bundy, F. P. Direct conversion of graphite to diamond in static pressure apparatus. *J. Chem. Phys.* **38,** 631–643 (1963).
2. Bundy, F. P. & Kasper, J. S. Hexagonal diamond—a new form of carbon. *J. Chem. Phys.* **46,** 3437–3446 (1967).
3. Bundy, F. P. *et al.* The pressure–temperature phase and transformation diagram for carbon; updated through 1994. *Carbon* **34,** 141–153 (1996).
4. Irifune, T., Kurio, A., Sakamoto, S., Inoue, T. & Sumiya, H. Ultrahard polycrystalline diamond from graphite. *Nature* **421,** 599–600 (2003).
5. Britun, V. F., Kurdyumov, A. V. & Petrusha, I. A. Diffusionless nucleation of lonsdaleite and diamond in hexagonal graphite under static compression. *Powder Metall. Met. Ceram.* **43,** 87–93 (2004).
6. Sumiya, H., Yusa, H., Inoue, T., Ofuji, H. & Irifune, T. Conditions and mechanism of formation of nano-polycrystalline diamonds on direct transformation from graphite and non-graphitic carbon at high pressure and temperature. *High Pressure Res.* **26,** 63–69 (2006).
7. Ohfuji, H. & Kuroki, K. Origin of unique microstructures in nano-polycrystalline diamond synthesized by direct conversion of graphite at static high pressure. *J. Mineral. Petrol. Sci.* **104,** 307–312 (2009).
8. Fahy, S., Louie, S. G. & Cohen, M. L. Pseudopotential total-energy study of the transition from rhombohedral graphite to diamond. *Phys. Rev. B* **34,** 1191–1199 (1986).
9. Fahy, S., Louie, S. G. & Cohen, M. L. Theoretical total-energy study of the transformation of graphite into hexagonal diamond. *Phys. Rev. B* **35,** 7623–7626 (1987).
10. Tateyama, Y., Ogitsu, T., Kusakabe, K. & Tsuneyuki, S. Constant-pressure first-principles studies on the transition states of the graphite–diamond transformation. *Phys. Rev. B* **54,** 14994–15001 (1996).
11. Scandolo, S., Bernasconi, M., Chiarotti, G. L., Focher, P. & Tosatti, E. Pressure-induced transformation path of graphite to diamond. *Phys. Rev. Lett.* **74,** 4015–4018 (1995).
12. Zipoli, F., Bernasconi, M. & Martonak, R. Constant pressure reactive molecular dynamics simulations of phase transitions under pressure: The graphite to diamond conversion revisited. *Eur. Phys. J. B* **39,** 41–47 (2004).
13. Khaliullin, R. Z., Eshet, H., Kühne, T. D., Behler, J. & Parrinello, M. Graphite–diamond phase coexistence study employing a neural-network mapping of the *ab initio* potential energy surface. *Phys. Rev. B* **81,** 100103 (2010).
14. Bundy, F. P., Strong, H. M., Bovenkerk, H. P. & Wentorf, R. H. Diamond–graphite equilibrium line from growth and graphitization of diamond. *J. Chem. Phys.* **35,** 383–391 (1961).
15. Bartok, A. P., Payne, M. C., Kondor, R. & Csanyi, G. Gaussian approximation potentials: The accuracy of quantum mechanics, without the electrons. *Phys. Rev. Lett.* **104,** 136403 (2010).
16. Mundy, C. J. *et al.* Ultrafast transformation of graphite to diamond: An *ab initio* study of graphite under shock compression. *J. Chem. Phys.* **128,** 184701 (2008).
17. Erskine, D. J. & Nellis, W. J. Shock-induced martensitic phase-transformation of oriented graphite to diamond. *Nature* **349,** 317–319 (1991).
18. Erskine, D. J. & Nellis, W. J. Shock-induced martensitic-transformation of highly oriented graphite to diamond. *J. Appl. Phys.* **71,** 4882–4886 (1992).
19. Vanderbilt, D. & Louie, S. G. Total energies of diamond (111) surface reconstructions by a linear combination of atomic orbitals method. *Phys. Rev. B* **30,** 6118–6130 (1984).

20. Zerilli, F. J. & Jones, H. D. Surface energy and the size of diamond crystals. *AIP Conf. Proc.* **370,** 163–166 (1996).
21. Bradley, R. S. Effect of pressure on rate of solid reactions, with special reference to diamond synthesis. *J. Inorg. Nucl. Chem.* **33,** 1969–1973 (1971).
22. Deryagin, B. V. & Fedoseev, D. V. Phase-transitions and nucleation in diamond and graphite. *Bull. Acad. Sci. USSR Div. Chem. Sci.* **28,** 1106–1109 (1979).
23. Behler, J. & Parrinello, M. Generalized neural-network representation of high-dimensional potential-energy surfaces. *Phys. Rev. Lett.* **98,** 146401 (2007).
24. Eshet, H., Khaliullin, R. Z., Kühne, T. D., Behler, J. & Parrinello, M. *Ab initio* quality neural-network potential for sodium. *Phys. Rev. B* **81,** 184107 (2010).
25. Yagi, T., Utsumi, W., Yamakata, M., Kikegawa, T. & Shimomura, O. High-pressure *in situ* X-ray-diffraction study of the phase-transformation from graphite to hexagonal diamond at room-temperature. *Phys. Rev. B* **46,** 6031–6039 (1992).
26. Chu, Y. A., Moran, B., Reid, A. C. E. & Olson, G. B. A model for nonclassical nucleation of solid–solid structural phase transformations. *Metall. Mater. Trans. A* **31,** 1321–1331 (2000).
27. Eshelby, J. D. The determination of the elastic field of an ellipsoidal inclusion, and related problems. *Proc. R. Soc. Lond. A* **241,** 376–396 (1957).
28. Le Guillou, C., Brunet, F., Irifune, T., Ohfuji, H. & Rouzaud, J. N. Nanodiamond nucleation below 2273 K at 15 GPa from carbons with different structural organizations. *Carbon* **45,** 636–648 (2007).
29. Suarez-Martinez, I., Savini, G., Haffenden, G., Campanera, J. M. & Heggie, M. I. Dislocations of Burgers vector c/2 in graphite. *Phys. Status Solidi C* **4,** 2958–2962 (2007).
30. Perdew, J. P., Burke, K. & Ernzerhof, M. Generalized gradient approximation made simple. *Phys. Rev. Lett.* **77,** 3865–3868 (1996).
31. Von Lilienfeld, O. A., Tavernelli, I., Rothlisberger, U. & Sebastiani, D. Optimization of effective atom centered potentials for London dispersion forces in density functional theory. *Phys. Rev. Lett.* **93,** 153004 (2004).

Acknowledgements

The authors would like to thank G. Tribello for reading the manuscript and M. Ceriotti for discussions. This work was supported by the European Research Council (ERC-2009-AdG-247075). J.B. is grateful for financial support from the FCI and the Deutsche Forschungsgemeinschaft. T.D.K. acknowledges support by the Graduate School of Excellence Mainz. Our thanks are also due to the Swiss National Supercomputing Centre and High Performance Computing Group of ETH Zürich for computer time.

Author contributions

R.Z.K. conceived the study, implemented the NN code, designed the NN potential, carried out simulations, analysed results and wrote the manuscript; H.E. designed and implemented the NN code, carried out simulations, contributed to the development of the NN potential and analysed results; T.D.K. analysed results and supervised the simulations; J.B. contributed to the implementation of the NN code and supervised the construction of the NN potential; M.P. conceived the study, analysed results, edited the manuscript and supervised the project.

Additional information

The authors declare no competing financial interests. Supplementary information accompanies this paper on www.nature.com/naturematerials. Reprints and permissions information is available online at http://www.nature.com/reprints. Correspondence and requests for materials should be addressed to R.Z.K.